LETTERS
PUBLISHED ONLINE: 26 JANUARY 2015 | DOI: 10.1038/NCLIMATE2498
nature climate change

Nonlinear regional warming with increasing CO_2 concentrations

Peter Good[1]*, Jason A. Lowe[1], Timothy Andrews[1], Andrew Wiltshire[1], Robin Chadwick[1], Jeff K. Ridley[1], Matthew B. Menary[1], Nathaelle Bouttes[2], Jean Louis Dufresne[3], Jonathan M. Gregory[1,2], Nathalie Schaller[4,5] and Hideo Shiogama[6]

When considering adaptation measures and global climate mitigation goals, stakeholders need regional-scale climate projections, including the range of plausible warming rates. To assist these stakeholders, it is important to understand whether some locations may see disproportionately high or low warming from additional forcing above targets such as 2 K (ref. 1). There is a need to narrow uncertainty[2] in this nonlinear warming, which requires understanding how climate changes as forcings increase from medium to high levels. However, quantifying and understanding regional nonlinear processes is challenging. Here we show that regional-scale warming can be strongly superlinear to successive CO_2 doublings, using five different climate models. Ensemble-mean warming is superlinear over most land locations. Further, the inter-model spread tends to be amplified at higher forcing levels, as nonlinearities grow—especially when considering changes per kelvin of global warming. Regional nonlinearities in surface warming arise from nonlinearities in global-mean radiative balance, the Atlantic meridional overturning circulation, surface snow/ice cover and evapotranspiration. For robust adaptation and mitigation advice, therefore, potentially avoidable climate change (the difference between business-as-usual and mitigation scenarios) and unavoidable climate change (change under strong mitigation scenarios) may need different analysis methods.

Linear assumptions affect stakeholder advice in various ways[1,3–7]. Fast simplified models[1,5,7] (especially integrated assessment models), for quantifying climate change under many policy scenarios, often assume that climate change is the same for each successive CO_2 doubling. Some studies make a less strong assumption: that regional climate is linear in global warming[3,4,6]. Also, studies of physical mechanisms often explore just one time period of one forcing scenario. An implied linear assumption here is that the physical mechanisms are similar under other scenarios or for other time periods, which is not necessarily true in a nonlinear system.

To quantify nonlinearities, the linear response must first be carefully defined. Even in a linear system the spatial patterns of climate change (per CO_2 doubling or per kelvin of global warming) can be different in different forcing scenarios or evolve during a given scenario. This is because of different timescales of response within the system[8–10]. For example, warming over the Southern Ocean lags the global mean[10]. Therefore, the spatial pattern of warming just after a CO_2 change is different from that several decades later.

Our experimental design is chosen to separate linear and nonlinear mechanisms. We use abruptCO_2 experiments, initialized from a pre-industrial control experiment. The CO_2 concentration is changed abruptly, then held constant for 150 years, revealing the model response over different timescales. The abrupt4×CO_2 experiment (with CO_2 quadrupled from pre-industrial levels) has similar forcing magnitude to a business-as-usual scenario by 2100 (ref. 11). The abrupt2×CO_2 experiment is identical to abrupt4×CO_2 but with half the CO_2 concentration (with forcing between that reached under Representative Concentration Pathway 2.6 (RCP2.6) and RCP4.5 scenarios by year 2100 (ref. 11)). A transient forcing experiment (1pctCO_2), where CO_2 is increased by 1% per year, is also used. We start with results from the HadGEM2-ES climate model.

The abruptCO_2 experiments are highly idealized. Therefore, we first show that their behaviour is comparable to the more policy-relevant 1pctCO_2 experiment, and detect nonlinearities in the 1pctCO_2 response. It is possible to use a simple linear combination of abruptCO_2 responses to estimate climate change under a transient forcing experiment[12,13]. This linear method performs well when the end of the 1pctCO_2 experiment (near 4×CO_2) is reconstructed from the abrupt4×CO_2 response (Fig. 1b). This shows that the abrupt4×CO_2 experiment features realistic physical mechanisms. It does not mean that temperature responses are linear (conceptually, it is like a local linear approximation to a curve). The importance of nonlinearity is revealed in the relatively poor performance when the abrupt2×CO_2 response is used instead (Fig. 1a); and for the middle of 1pctCO_2 (near 2×CO_2), the reconstruction using abrupt4×CO_2 is much worse than that using abrupt2×CO_2 (compare Fig. 1c,d). The linear method is accurate only for periods in the transient experiment with forcing matching that of the abruptCO_2 experiment: climate patterns are therefore different for different CO_2 concentrations—which is evidence of nonlinearity.

Having detected nonlinearities in the 1pctCO_2 experiment, we characterize them more clearly by analysing the abruptCO_2 experiments directly. This experimental design has two significant advantages over the 1pctCO_2 scenario. First, temperature responses in the two abruptCO_2 experiments may be compared at the same timescale after CO_2 is changed (eliminating complications due to linear effects from different timescales of response). Second, noise

[1]Met Office Hadley Centre, Exeter EX1 3PB, UK. [2]NCAS-Climate, University of Reading, Reading RG6 6AH, UK. [3]Laboratoire de Météorologie Dynamique, Institut Pierre Simon Laplace, 75005 Paris, France. [4]Institute for Atmospheric and Climate Science, Department of Environmental Sciences, ETH Zurich, CH-8092 Zurich, Switzerland. [5]Atmospheric, Oceanic and Planetary Physics, University of Oxford, Parks Road, Oxford OX1 3PU, UK. [6]Climate Risk Assessment Section, Centre for Global Environmental Research, National Institute for Environmental Studies, Tsukuba 305-8506, Japan.
*e-mail: peter.good@metoffice.gov.uk

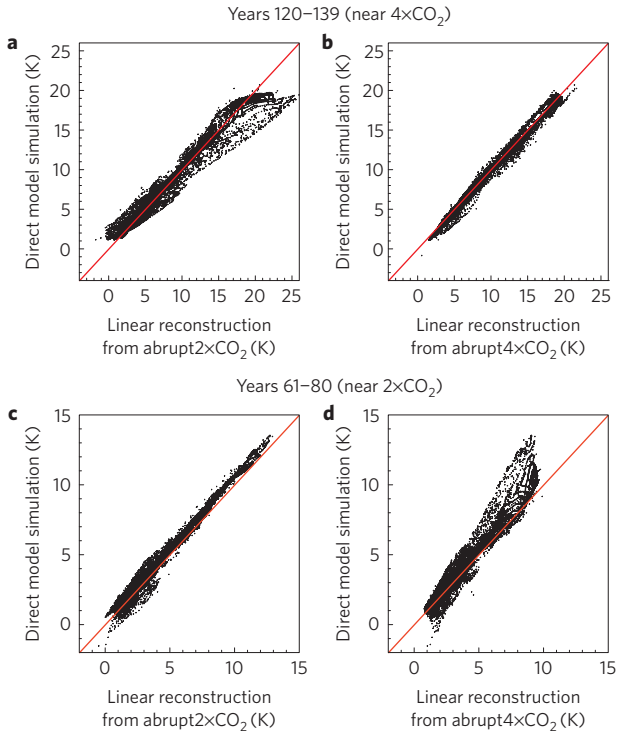

Figure 1 | Regional nonlinearity in the transient-forced 1pctCO$_2$ experiment. a–d, Warming simulated directly by HadGEM2-ES (*y* axis) is compared with that predicted from the linear reconstruction[12,13] using abrupt2×CO$_2$ (left column) and abrupt4×CO$_2$ (right column) responses. Good performance of the linear reconstruction is indicated by the points lying close to the red line (each point represents one model grid cell). Results are averaged over years 120–139 of the 1pctCO$_2$ experiment (near 4×CO$_2$; top row), and years 61–80 (near 2×CO$_2$; bottom row).

from internal variability may be reduced through long-term means. Assuming that the balance of mechanisms should be stable after the initial ocean mixed-layer warming, we average over years 50–149 of each experiment (Supplementary Fig. 1). For abrupt2×CO$_2$, these 100-year means correspond roughly to the results for year 2100 of a CO$_2$-only version of RCP4.5 (Supplementary Methods; and about double this for abrupt4×CO$_2$).

We compare temperature responses to a first and second CO$_2$ doubling. Current linear methods that parameterize forcing (most integrated assessment and energy balance models) assume that radiative forcing is linear in log(CO$_2$)—and equivalently, that each CO$_2$ doubling produces the same forcing change[1,5]. In HadGEM2-ES, the two doublings give very similar forcing changes[14]. The response to the first doubling is given by abrupt2×CO$_2$ minus the pre-industrial control; that for the second doubling by abrupt4×CO$_2$ minus abrupt2×CO$_2$ (both are averaged over years 50–149). We quantify nonlinearities by the 'doubling difference': the response to the second doubling minus that for the first (Fig. 2a); and the 'doubling ratio': the second doubling divided by the first (Fig. 2b). Current linear models would have zero doubling difference, and a doubling ratio of 1, everywhere.

In HadGEM2-ES, the doubling ratio in global-mean warming is 1.18 (the second CO$_2$ doubling produces more warming than the first). Global-scale nonlinearity has been attributed, in other models, to changes in water-vapour and cloud feedbacks, opposed by changes in albedo and lapse-rate feedbacks[15–17]. In some climate models, variation in forcing per CO$_2$ doubling would also affect the global doubling ratio[15–17]. However, local doubling ratios can differ significantly from the global mean: 5% of the land surface has a doubling ratio outside the range 0.9–1.65 (Supplementary Fig. 5a). Gradients of the doubling ratio across continents are strong (Fig. 2b), notably over the Americas and Europe, pointing to important regional mechanisms.

We scale out global-mean nonlinearity (Methods) and then focus on the remaining features (Fig. 2c) one by one. The positive area in the North Atlantic, near Greenland, seems to be associated with a nonlinear response of the Atlantic meridional overturning circulation[18] (AMOC). In HadGEM2-ES, the maximum Atlantic overturning near 30° N weakens about 35% less under a second CO$_2$ doubling than under the first (a positive doubling difference). We can estimate the effect on surface temperature by scaling the regional temperature response in a separate freshwater hosing experiment (where fresh water is added to the high-latitude North Atlantic to induce AMOC weakening). We multiplied this temperature response pattern by the ratio: (doubling difference for AMOC index)/(AMOC index response in the hosing experiment). The resulting pattern (Fig. 2d) features a North Atlantic anomaly similar to that in Fig. 2c. This suggests that the North Atlantic nonlinearity is indeed driven by the nonlinear AMOC response. AMOC nonlinearity may arise from variation in the salt-advection feedback (which affects the AMOC strength)[19]. The AMOC transports heat to the North Atlantic, so a positive doubling difference in the AMOC causes positive doubling differences in North Atlantic surface temperatures.

To reveal other nonlinear mechanisms, we subtract the AMOC pattern (Fig. 2d) from that in Fig. 2c. The residual (Fig. 2e) is associated with mechanisms other than those in the global-mean energy balance or the AMOC. The North Atlantic positive feature has been effectively removed.

The remaining high-latitude temperature nonlinearities are largely driven by a nonlinear albedo feedback[18,20] (which is dominated by changes in ice and snow cover). It is nonlinear[21] as it becomes zero when ice/snow is either absent or so thick that its extent changes little under warming. The patterns in the doubling difference of sea-ice fraction (Fig. 2f) match closely the high-latitude patterns of temperature doubling difference (Fig. 2e), with sea-ice albedo feedbacks driving temperature nonlinearity (Supplementary Methods).

The final mechanism we study involves land evapotranspiration. Soil moisture–temperature feedbacks can be nonlinear[22]: feedback is small when soil moisture is saturated, or so low that moisture is tightly bound to the soil (in both regimes, evaporation is insensitive to change in soil moisture)[23]. Nonlinear behaviour could also occur through the response of plant stomata (and hence transpiration) to increased CO$_2$ (ref. 24), or through nonlinear precipitation change[25,26]. In HadGEM2-ES, the most strongly superlinear warming occurs over the Amazon (doubling ratios of 80% are driven by the response of forest tree stomata to CO$_2$, with a longer-term response from reduced vegetation productivity—Supplementary Methods; Amazon nonlinearity is weaker in the other models studied). To investigate this type of effect, we calculate the ratio of mean surface sensible heat and mean surface latent heat fluxes (the Bowen ratio) in the two abruptCO$_2$ experiments. Much of the temperature nonlinearity over mid/low-latitude land (Fig. 2g) is associated with change in the Bowen ratio (Fig. 2h). Regions where the Bowen ratio is substantially larger at 4×CO$_2$ than at 2×CO$_2$ (red in Fig. 2h) have more restricted evaporation: more incident heat is lost as sensible heat, causing further warming. This does not occur where the Bowen ratio is already larger than 1 at 2×CO$_2$ (for example, the Sahara, where most turbulent heat is sensible even at 2×CO$_2$). These regions are masked in Fig. 2h.

Further to our analysis of HadGEM2-ES we find that nonlinearity is similarly important in four other climate models: NCAR CESM1, IPSL CM5A-LR, MIROC5 T42 and HadCM3. These models show doubling ratios over land comparable to those in HadGEM2-ES (Supplementary Fig. 5a). Over most land locations,

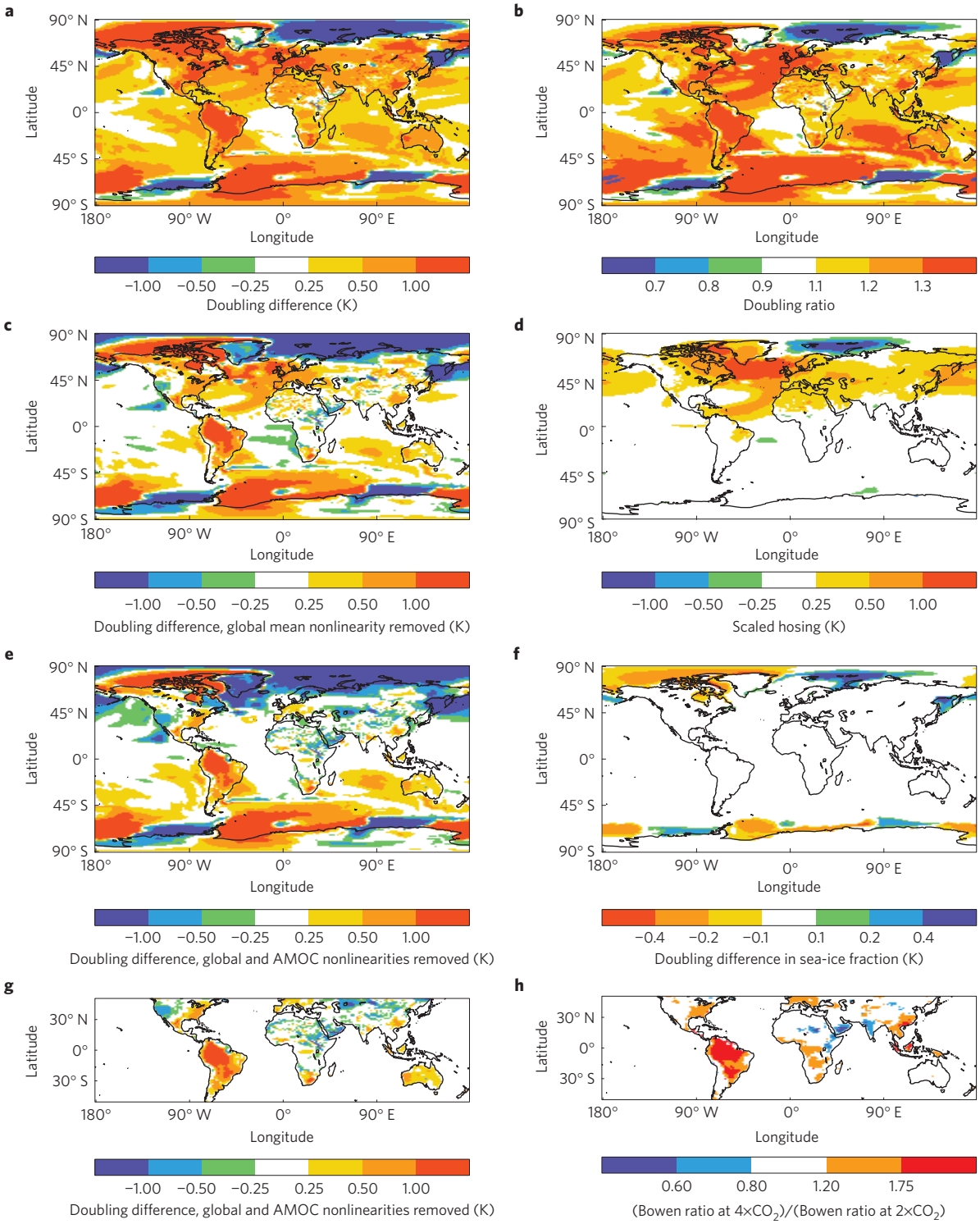

Figure 2 | Mechanisms of nonlinear regional warming in HadGEM2-ES. a, Doubling difference. **b**, Doubling ratio. **c**, Doubling difference after global-mean nonlinearity is scaled out (Methods). **d**, Estimated nonlinearity associated with the AMOC. **e**, The same as in **c** but with nonlinearity associated with the AMOC (**d**) subtracted. **f**, Doubling difference in sea-ice fraction. **g**, The same as in **e** but latitude range matches that of **h**. **h**, Bowen ratio at $4\times CO_2$ divided by Bowen ratio at $2\times CO_2$. All based on means over years 50–149 of the abrupt$2\times CO_2$, abrupt$4\times CO_2$ or hosing experiments, using HadGEM2-ES.

the ensemble-mean doubling difference is comparable to the ensemble standard deviation for warming from the first doubling (Supplementary Fig. 5b). That is, the range of warmings simulated by this ensemble is quite different for the first and second CO_2 doublings. The models do show differences in spatial patterns of nonlinear warming. Consequently, the ensemble-mean pattern (Fig. 3) is smoother than that of any individual model. However, some continental-scale patterns across Europe, North and South America and tropical Africa are similar between Figs 2b and 3.

Nonlinearity has implications not just for the ensemble mean, but also for the spread of model projections. In general, an increased spread at higher forcing should be expected: the relative importance

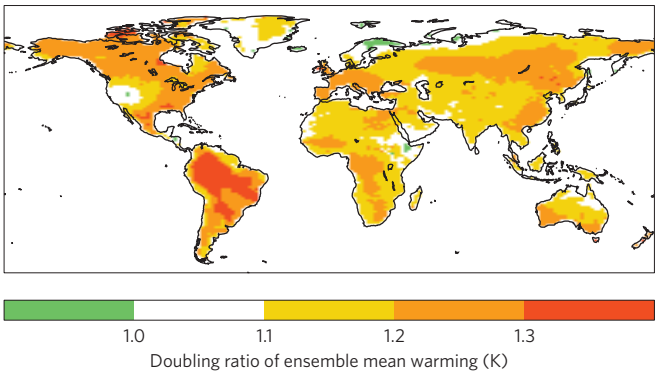

Figure 3 | Doubling ratio of ensemble-mean warming. Ensemble means are taken for each of the first and second CO_2 doublings first; then the doubling ratio is calculated.

of nonlinear mechanisms grows with increasing forcing, so their contribution to model spread does likewise. Conceptually, this can be thought of as including an extra uncertain process at higher CO_2 concentrations. This inflation in model spread at higher forcing is large when nonlinearities are uncertain, and seems to be especially relevant for change per kelvin of global warming. We calculated the ensemble standard deviation in regional warming per kelvin of global warming. Over 30% of land, the ensemble spread is at least 40% larger for the second doubling than for the first doubling (not driven by internal variability—Supplementary Methods). This corresponds to a doubling of variance—driven by uncertain nonlinear mechanisms. This implies that the additional regional warming under a business-as-usual scenario (over and above that in a mitigation scenario) may be more uncertain than the warming under a mitigation scenario—a fact missed by previous linear impacts assessments[1,3,4]. Second, different techniques may be needed to reduce model uncertainty in these two aspects of climate change: uncertainty from nonlinear mechanisms being relatively more important at higher than at lower forcing levels.

The mechanisms of nonlinear warming identified in HadGEM2-ES also operate in the other four models studied. All have a positive global-mean temperature nonlinearity (Supplementary Table 1). As done for HadGEM2-ES, we scale this global-mean nonlinearity out and discuss regional patterns. Most of the remaining temperature nonlinearities over northwest Europe are associated with the AMOC: the magnitude of this nonlinearity is predicted simply by scaling the HadGEM2-ES hosing experiment by the AMOC doubling difference from each model (Fig. 4a). Although there is significant model spread in sea-ice nonlinearity (Supplementary Fig. 6), Arctic temperature doubling differences averaged across the four extra models align closely with the sea-ice albedo doubling differences (Fig. 4b,c), with patterns similar to those for HadGEM2-ES (Fig. 2f). Similar comments apply to the evaporation mechanism at lower latitudes (Fig. 4d,e and Supplementary Fig. 7), especially over the Americas, Africa and Arabia, although not all of the pattern is explained this way (nonlinear dynamical processes and internal variability may also contribute).

The implications of nonlinearity for individual studies will be application-specific, and should be considered alongside other issues (for example, uncertainty in impacts models). Further differences in patterns of 'potentially avoidable' and 'unavoidable' warming may arise from linear mechanisms. The abruptCO_2 experiments are powerful for separating mechanisms and identifying where nonlinearity is largest or smallest. Where available, transient projections from state-of-the-art climate models remain preferable for direct policy advice.

Work is needed to reduce uncertainty in these nonlinear mechanisms. Results from more models are required to quantify

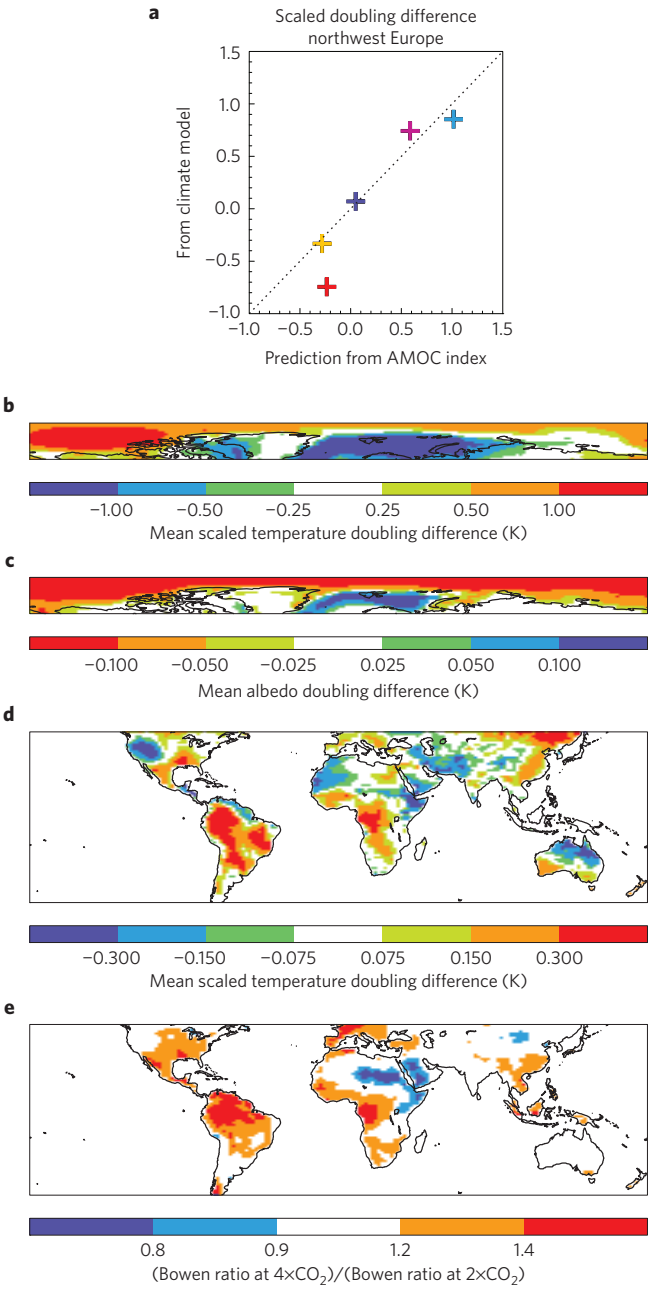

Figure 4 | Multi-model mechanisms of temperature nonlinearity. All panels: 'scaled temperature doubling differences' have had the global-mean nonlinearity scaled out. **a**, AMOC influence, averaged over northwest Europe (land, 10° W–20° E, 45–70° N). *y* axis: scaled temperature doubling difference for each model; *x* axis: the HadGEM2-ES hosing temperature response scaled using the doubling difference in AMOC index for each model (as Fig. 2d; pink: HadGEM2-ES; dark blue: HadCM3; light blue: MIROC5; yellow: NCAR CESM1; red: IPSL CM5A-LR). **b**,**c**, Sea-ice influence. Ensemble means (excluding HadGEM2), of scaled temperature doubling difference (**b**) and albedo doubling difference (**c**). **d**,**e**, Evaporation influence. **d**, Ensemble-mean (excluding HadGEM2) scaled temperature doubling difference. **e**, Bowen ratio of ensemble-mean surface heat fluxes at $4\times CO_2$, divided by the equivalent at $2\times CO_2$ (as Fig. 2h).

model spread more precisely. Some policy advice based on linear methods[3] may need to be reconsidered, and studies of physical processes controlling both temperature and precipitation[25,26] should account for a different balance of mechanisms under different forcing scenarios or for different time periods.

Methods

HadGEM2-ES model and experiments. The Hadley Centre Global Environmental Model version 2 Earth System configuration[27,28] (HadGEM2-ES) has an atmospheric resolution of 1.25 × 1.875° and 38 vertical levels, and a 1° ocean (reaching 1/3° near the Equator) with 40 vertical levels. NCAR CESM1, HadCM3, IPSL CM5A-LR and MIROC5 are described in Supplementary Table 2.

All models ran a fixed-forcings pre-industrial control, and both abruptCO_2 experiments. Each abruptCO_2 experiment was initialized from the same point in the control run, and CO_2 was abruptly changed (to twice pre-industrial levels for abrupt2×CO_2 and four times for abrupt4×CO_2), and then held constant for 150 years.

The hosing experiment, run only for HadGEM2-ES, involved addition of 0.1 Sv fresh water near the coast of Greenland for 100 years. This produced a modest (30%) slowdown in the AMOC (measured by maximum overturning near 30° N). Results from this experiment were averaged over years 50–149.

Scaling the global-mean nonlinearity out. Figure 2c shows doubling differences after the global-mean nonlinearities (except those due to the AMOC) are scaled out. The calculation of doubling differences with global nonlinearities scaled out (denoted $DD_{noglobal}$) is described below. The small global-mean nonlinearity associated with the AMOC is not scaled out here. This is because the global-mean AMOC effect is included in Fig. 2d (the scaled hosing response), and is therefore removed when Fig. 2d is subtracted from Fig. 2c: to give the residual in Fig. 2e. $DD_{noglobal}$ is given by:

$$DD_{noglobal} = T_{42} - T_{21,scaled}$$

where T_{42} is the warming from the second doubling, and:

$$T_{21,scaled} = T_{21} \cdot \frac{\left(\overline{T_{21}} + \overline{DD_{noAMOC}}\right)}{\overline{T_{21}}}$$

where T_{21} is the warming from the first doubling. The overbar indicates a global mean. $\overline{DD_{noAMOC}}$ is the global-mean doubling difference from processes other than the AMOC:

$$\overline{DD_{noAMOC}} = \overline{DD} - \overline{DD_{AMOC}}$$

$\overline{DD}$ is the global mean of Fig. 2a and DD_{AMOC} is the global mean of Fig. 2d.

Received 17 July 2014; accepted 12 December 2014; published online 26 January 2015; corrected after print 28 January 2015

References

1. Arnell, N. W. *et al.* A global assessment of the effects of climate policy on the impacts of climate change. *Nature Clim. Change* **3,** 512–519 (2013).
2. Oppenheimer, M. Defining dangerous anthropogenic interference: The role of science, the limits of science. *Risk Anal.* **25,** 1399–1407 (2005).
3. Gosling, S. N. *et al.* A review of recent developments in climate change science. Part II: The global-scale impacts of climate change. *Prog. Phys. Geogr.* **35,** 443–464 (2011).
4. Todd, M. C. *et al.* Uncertainty in climate change impacts on basin-scale freshwater resources—preface to the special issue: The QUEST-GSI methodology and synthesis of results. *Hydrol. Earth Syst. Sci.* **15,** 1035–1046 (2011).
5. Van Vuuren, D. P. *et al.* How well do integrated assessment models simulate climate change? *Climatic Change* **104,** 255–285 (2011).
6. Moss, R. H. *et al.* The next generation of scenarios for climate change research and assessment. *Nature* **463,** 747–756 (2010).
7. Huntingford, C. *et al.* Simulated resilience of tropical rainforests to CO_2-induced climate change. *Nature Geosci.* **6,** 268–273 (2013).
8. Chadwick, R., Wu, P. L., Good, P. & Andrews, T. Asymmetries in tropical rainfall and circulation patterns in idealised CO_2 removal experiments. *Clim. Dynam.* **40,** 295–316 (2013).
9. Li, S. & Jarvis, A. Long run surface temperature dynamics of an A-OGCM: The HadCM3 4×CO_2 forcing experiment revisited. *Clim. Dynam.* **33,** 817–825 (2009).
10. Manabe, S., Bryan, K. & Spelman, M. J. Transient-response of a global ocean atmosphere model to a doubling of atmospheric carbon-dioxide. *J. Phys. Oceanogr.* **20,** 722–749 (1990).
11. Meinshausen, M. *et al.* The RCP greenhouse gas concentrations and their extensions from 1765 to 2300. *Climatic Change* **109,** 213–241 (2011).
12. Good, P., Gregory, J. M. & Lowe, J. A. A step-response simple climate model to reconstruct and interpret AOGCM projections. *Geophys. Res. Lett.* **38,** L01703 (2011).
13. Good, P., Gregory, J. M., Lowe, J. A. & Andrews, T. Abrupt CO_2 experiments as tools for predicting and understanding CMIP5 representative concentration pathway projections. *Clim. Dynam.* **40,** 1041–1053 (2013).
14. Andrews, T. & Ringer, M. A. Cloud feedbacks, rapid adjustments, and the forcing-response relationship in a transient CO_2 reversibility scenario. *J. Clim.* **27,** 1799–1818 (2014).
15. Jonko, A. K., Shell, K. M., Sanderson, B. M. & Danabasoglu, G. Climate feedbacks in CCSM3 under changing CO_2 forcing. Part II: Variation of climate feedbacks and sensitivity with forcing. *J. Clim.* **26,** 2784–2795 (2013).
16. Colman, R. & McAvaney, B. Climate feedbacks under a very broad range of forcing. *Geophys. Res. Lett.* **36,** L01702 (2009).
17. Hansen, J. *et al.* Efficacy of climate forcings. *J. Geophys. Res.* **110,** D18104 (2005).
18. Ishizaki, Y. *et al.* Temperature scaling pattern dependence on representative concentration pathway emission scenarios. *Climatic Change* **112,** 535–546 (2012).
19. Drijfhout, S. S., Weber, S. L. & van der Swaluw, E. The stability of the MOC as diagnosed from model projections for pre-industrial, present and future climates. *Clim. Dynam.* **37,** 1575–1586 (2011).
20. Hall, A. The role of surface albedo feedback in climate. *J. Clim.* **17,** 1550–1568 (2004).
21. Eisenman, I. Factors controlling the bifurcation structure of sea ice retreat. *J. Geophys. Res.* **117,** D01111 (2012).
22. Seneviratne, S. I. *et al.* Investigating soil moisture-climate interactions in a changing climate: A review. *Earth-Sci. Rev.* **99,** 125–161 (2010).
23. Seneviratne, S. I., Luthi, D., Litschi, M. & Schar, C. Land-atmosphere coupling and climate change in Europe. *Nature* **443,** 205–209 (2006).
24. Field, C. B., Jackson, R. B. & Mooney, H. A. Stomatal responses to increased CO_2—implications from the plant to the global-scale. *Plant Cell Environ.* **18,** 1214–1225 (1995).
25. Chadwick, R. & Good, P. Understanding non-linear tropical precipitation responses to CO_2 forcing. *Geophys. Res. Lett.* **40,** 4911–4915 (2013).
26. Good, P. *et al.* A step-response approach for predicting and understanding non-linear precipitation changes. *Clim. Dynam.* **39,** 2789–2803 (2012).
27. Collins, W. J. *et al.* Development and evaluation of an Earth-System model—HadGEM2. *Geosci. Model Dev.* **4,** 1051–1075 (2011).
28. Martin, G. M. *et al.* The HadGEM2 family of Met Office Unified Model climate configurations. *Geosci. Model Dev.* **4,** 723–757 (2011).

Acknowledgements

This work was supported by the Joint UK DECC/Defra Met Office Hadley Centre Climate Programme (GA01101). N.B. and J.M.G. received financial support from the European Research Council under the European Community's Seventh Framework Programme (FP7/2007–2013), ERC Grant Agreement 247220, project 'Seachange'. Simulations by J.L.D. were performed as part of the ANR ClimaConf project (grant no. ANR-10-CEPL-0003). H.S. was supported by the SOUSEI program from the Ministry of Education, Culture, Sports, Science and Technology of Japan and the Environment Research and Technology Development Fund (S-10) of the Ministry of the Environment of Japan. N.S. was supported by the Swiss National Science Foundation.

Author contributions

P.G. conceived the study and wrote the paper. All authors contributed to the scientific interpretation and the paper. T.A., M.B.M., J.L.D., J.M.G., N.S. and H.S. performed experiments.

Additional information

Supplementary information is available in the online version of the paper. Reprints and permissions information is available online at www.nature.com/reprints. Correspondence and requests for materials should be addressed to P.G.

Competing financial interests

The authors declare no competing financial interests.

CORRIGENDUM

Nonlinear regional warming with increasing CO_2 concentrations

Peter Good, Jason A. Lowe, Timothy Andrews, Andrew Wiltshire, Robin Chadwick, Je-K. Ridley, Matthew B. Menary, Nathaelle Bouttes, Jean Louis Dufresne, Jonathan M. Gregory, Nathalie Schaller and Hideo Shiogama

Nature Clim. Change **5,** 138–142 (2015); published online 26 January 2015; corrected after print 28 January 2015

In the version of this Letter originally published, the fourth author affiliation should have read '[4]Institute for Atmospheric and Climate Science, Department of Environmental Sciences, ETH Zurich, CH-8092 Zurich, Switzerland.' This error has been corrected in the online versions of the Letter.